

# PERSON REIDENTIFICATION USING QUATERNIONIC LOCAL BINARY PATTERN

*Rushi Lan, Yicong Zhou, Yuan Yan Tang, C. L. Philip Chen*

Department of Computer and Information Science, University of Macau, Macau 999078, China  
{rslan, yicongzhou, yytang, philipchen}@umac.mo

## ABSTRACT

Person reidentification is to identify the persons observed in nonoverlapping camera networks. Most existing methods usually extract features from the red, green, and blue color channels of images individually. They, however, neglect the connections between each color component in the image. To overcome this problem, a novel quaternionic local binary pattern (QLBP) is proposed for person reidentification in this paper. In the proposed QLBP, each pixel in a color image is represented by a quaternion so that we can handle all color components in a holistic way. A novel pseudo-rotation of quaternion (PRQ) is proposed to rank two quaternions. Some properties of PRQ are also discussed. After a QLBP coding, the local histograms are extracted and used as features. Experiments on two public benchmarking datasets, ETHZ and i-LIDS MCTS, are carried out to evaluate the QLBP performance. Comparison results show that the QLBP outperforms several stat-of-art methods for person reidentification.

**Index Terms**— Person reidentification, quaternion, local binary pattern, feature extraction

## 1. INTRODUCTION

Nowadays, more and more visual surveillance systems are applied in many public places for a security purpose, such as the shopping malls, waiting halls for airplanes, or railway stations, etc. In these cases, the video data are usually obtained from nonoverlapping camera networks. Therefore, it is a critical problem to identify a person from disjoint camera views at different locations, which is known as person reidentification and has been extensively studied recently [1, 2].

The person reidentification is a hard problem and still largely unsolved. The main reason may lie in that there usually exists a great variance of a person's appearance in different images obtained by different nonoverlapping cameras. Fig. 1 shows some example images captured from real complex environments. Images in each column contain the same person. We can find that it is difficult to decide whether two images

---

This work was supported in part by the Macau Science and Technology Development Fund under Grant 106/2013/A3, and by the Research Committee at University of Macau under Grants MYRG113(Y1-L3)-FST12-ZYC and MRG001/ZYC/2013/FST.

are with the same person due to the synthetic effects of the view angle, lighting, occlusion, and background clutter, etc.

A person reidentification system is usually composed of two parts, namely feature representation and distance based determination. In this paper, we focus on the first part. Many efforts have been devoted to extract features for person reidentification. These approaches can be roughly divided into two categories: global-based and local-based methods.

In global-based methods, all pixels in the image are taken into account to get the appearance representation. Examples like the dense color histogram, Zheng's method [1], dense SIFT [3], and histogram of oriented gradient (HOG) descriptor [4], etc. The main advantage of these methods is that it gives an overall description of the original image. On the other hand, local-based methods subdivide the human body into several parts, then extract features from each part [5, 6]. This type of methods offers more detailed local information for person reidentification.

The images captured by the surveillance cameras are usually color images represented in the RGB color space. To describe these images, features are extracted from each color channel component respectively, and simply combined together. It is well known that there exist important relations between each color channel component [7]. However, the aforementioned methods neglect these relations which maybe greatly improve the classification performance. To process the color image components in a holistic way, Sangwine put forward the idea of using the quaternion number to represent the color image pixel [8]. Since then, the quaternion numbers have been successfully adopted to all kinds of color image processing tasks, including image smoothing and segmentation, denoising, object reconstruction, image quality evaluation, and recognition, etc.

On the other hand, the well-known local binary pattern (LBP), first proposed by Ojala *et al.* [9], is a simple but efficient tool to describe the local information within an image. It has been proved to be robust to different variations (like illumination, view angle, pose, and occlusion) in texture classification and face recognition. Therefore, it is worthwhile to use LBP to address the person reidentification problem. However, if we directly perform LBP to each color channel respectively or just to the luminance component, the relations between each color channel component are ignored.

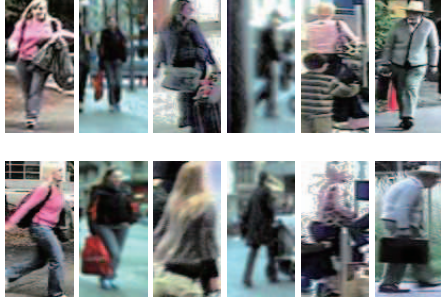


**Fig. 1:** Person image examples of appearance changes.

In this paper, a novel quaternionic local binary pattern (QLBP) is proposed for person reidentification. We first utilize the quaternion number to represent each color image pixel, and then extract LBP features based on the quaternionic representation. Consequently, the obtained features integrate advantages of both the quaternionic representation and LBP such that they can be used to address the person reidentification problem well. In summary, our main contributions can be listed as follows:

1. To the best of our knowledge, this is the first time to use quaternion representation to address the person reidentification problem.
2. We develop a novel pseudo-rotation of quaternion (PRQ) to rank two quaternions, and discuss its properties.
3. A quaternionic local binary pattern (QLBP) histogram method is proposed for person reidentification, which is simple and easy to implement.

## 2. PRELIMINARY

### 2.1. Quaternion

The quaternion, introduced by Hamilton in 1843 [10], is a four-dimensional generalization of the complex number with one real part and three imaginary parts. It can be represented in a complex form as follows:

$$q = a + ib + jc + kd, \quad (1)$$

where  $a, b, c$  and  $d$  are real numbers,  $i, j$  and  $k$  are complex operators, and they satisfy:

$$i^2 = j^2 = k^2 = ijk = -1.$$

$a$  is called the real part of a quaternion, and  $ib + jc + kd$  is called the imaginary part. Denote the real part and imaginary part as  $S(q)$  and  $V(q)$  respectively, then it has  $q = S(q) + V(q)$ .

Usually, we apply its imaginary part of the quaternion to represent a color pixel, namely

$$q = ir + jg + kb, \quad (2)$$

where  $r, g$ , and  $b$  are red, green, and blue components of the color pixel respectively.

Several properties of complex numbers have been extended to the quaternion. Some of them are as follows:

- Conjugate:  $\bar{q} = a - (ib + jc + kd)$ ;
- A pure quaternion:  $q = ib + jc + kd$ ;
- Modulus:  $|q| = \sqrt{q\bar{q}} = \sqrt{\bar{q}q} = \sqrt{a^2 + b^2 + c^2 + d^2}$ ;
- Inverse:  $q^{-1} = \frac{\bar{q}}{|q|^2}$  so that  $qq^{-1} = 1$ ;
- Noncommutativity of multiplication:  $ij = -ji = k, kj = -kj = i, ki = -ik = j$ .

As complex number, any quaternion also can be represented in polar form:

$$q = |q|e^{\mu\theta} = |q|(\cos\theta + \mu\sin\theta), \quad (3)$$

where  $\mu$  is a unit pour quaternion, and  $0 \leq \theta \leq \pi$ .  $\mu$  and  $\theta$  are known as the eigenaxis and phase (or eigenangle ) of the quaternion, which can be obtained by:

$$\mu = \frac{V(q)}{|V(q)|}, \quad \theta = \tan^{-1} \frac{|V(q)|}{S(q)}.$$

Rotation is an important operation of the quaternion. The definition is given as following.

**Definition 1 (Rotation of Quaternion, RQ):** The rotation of the quaternion  $q$  by a unit quaternion  $p$  is defined by:

$$RQ(q, p) = pq\bar{p}. \quad (4)$$

The real part of  $q$  does not change, but its imaginary part is rotated in a three dimensional (3D) space.

### 2.2. Local binary pattern (LBP)

The image local differences can be decomposed into two parts: the sign and magnitude [11]. The traditional LBP makes use of the sign part to code the local pattern as an 8-digit binary number, which is usually converted to decimal for convenience. Let  $x_i$  be the center pixel of a  $3 \times 3$  block  $S_i$  within a grayscale image, LBP coding is obtained by comparing  $x_i$  with its surrounding pixels as following:

$$LBP_{x_i} = \sum_{j=0}^{|S_i|-1} h(x_j - x_i)2^j, \quad h(t) = \begin{cases} 1, & t \geq 0. \\ 0, & t < 0. \end{cases} \quad (5)$$

where  $|S_i|$  is the number of elements in  $S_i$ . Then a histogram can be computed over an image cell and used as features of the image.

### 3. QUATERNIONIC LOCAL BINARY PATTERN

In this section, we first introduce a ranking function of two quaternions and pseudo-rotation of quaternion (PRQ). Combining them together, we propose the quaternionic ranking with PRQ. We finally introduce a new quaternionic local binary pattern (QLBP).

#### 3.1. Ranking of two quaternions

LBP coding can be transferred into a ranking problem. We define a ranking function of  $x_i$  and  $x_j$  as  $R(x_i, x_j)$ . If  $x_j$  is ranked higher than  $x_i$ ,  $R(x_i, x_j) \geq 0$ , else  $R(x_i, x_j) < 0$ . This concept can be applied to the quaternionic representation of a color image. Suppose  $q_i$  and  $q_j$  are two quaternions representing the centering and surrounding pixels in a color image, the ranking function  $R(q_i, q_j)$  is used to rank  $q_i$  and  $q_j$ . Next, we discuss how to find an appropriate  $R(q_i, q_j)$ .

A natural idea is to use the modulus of the difference between two quaternions, namely

$$R(q_i, q_j) = |q_j - q_i|. \quad (6)$$

Since  $R(x_i, x_j)$  is not less than zero, it is difficult to find a proper threshold to determine the ranking between two quaternions.

Another option is to compare the modulus of two quaternions as following

$$R(q_i, q_j) = |q_j| - |q_i|. \quad (7)$$

But the above  $R(q_i, q_j)$  is lack of discriminative ability.

Except for using the modulus, the phase of the quaternion can also be used to rank two quaternions because it reveals the relationship between the real and imaginary parts of a quaternion. If we represent the color pixel using Eq. (2), the phase is equal to  $\pi$  for all pixels.

From the above discussion, it is difficult to rank two quaternions just using their moduli or phases. To overcome this obstacle, we introduce a reference quaternion. Because the quaternion is a hypercomplex representation of the color image, we rotate two quaternions by the reference quaternion, and then rank two quaternions according to their new phases or moduli. There are at least two advantages using this rotation:

1. We can obtain an explicit ranking decision for two quaternions rotated by a given reference one;
2. Changing the reference quaternion yields a complete ranking decision.

However, the rotation in Define 1 cannot achieve these purposes because the modulus and phase of a quaternion keep the same after rotation. Therefore, we need to find a novel “rotation” for quaternion which will be introduced in the following section.

#### 3.2. Pseudo-rotation of quaternion (PRQ)

This subsection proposes a novel rotation of quaternion, called the pseudo-rotation of quaternion (PRQ). Its definition is given as following:

**Definition 2 (Pseudo-Rotation of Quaternion, PRQ):**

Suppose  $q$  is a quaternion, and  $p$  is a unit quaternion. The right and left pseudo-rotation of  $q$  by  $p$  are defined as following respectively:

$$\text{PRQ}_r(q, p) = qp \text{ and } \text{PQR}_l(q, p) = pq. \quad (8)$$

Based on the PRQ definition and properties of the quaternion, we can derive the following properties of PRQ.

**Property 1** The PRQ does not change the modulus of the quaternion, namely

$$|q| = |\text{PRQ}_r(q, p)| = |\text{PQR}_l(q, p)|. \quad (9)$$

**Property 2** Due to the noncommutativity of multiplication,  $\text{PRQ}_r(q, p)$  is not equal  $\text{PQR}_l(q, p)$ , but their phases are the same, namely

$$\theta_{\text{PRQ}_r(q, p)} = \theta_{\text{PQR}_l(q, p)}. \quad (10)$$

For simplicity, we use  $\theta_{\text{PQR}(q, p)}$  to represent the phase of both right and left pseudo-rotation of  $q$  about  $p$ .

**Property 3** If  $q$  and  $p$  are both unit quaternions, the right pseudo-rotation of  $q$  along  $p$  is equivalent to the left pseudo-rotation of  $p$  along  $q$ , namely

$$\text{PRQ}_r(q, p) = \text{PQR}_l(p, q). \quad (11)$$

**Property 4** The rotation of a quaternion  $q$  along another unit quaternion  $p$  can be obtained by a combination of left and right pseudo-rotation of  $q$  and  $p$  as following:

$$\begin{aligned} \text{RQ}(q, p) &= \text{PRQ}_r(\text{PQR}_l(q, p), \bar{p}) \\ &= \text{PRQ}_l(\text{PQR}_r(q, \bar{p}), p). \end{aligned} \quad (12)$$

#### 3.3. Quaternionic ranking with PRQ

Since the PRQ keeps the modulus of the quaternion unchanged (See Property 1), the only thing can be used to rank the quaternions is the phase of the PRQ. One may ask that can the phase of a PRQ explicitly rank two quaternions well? Next, we will explain this point in detail.

For simplicity, let  $q = ir + jg + kb$  and  $p = ix + jy + kz$ , where  $r, g$ , and  $b$  are intensity values of the red, green, and blue components of a pixel in a color image, and  $p$  is a unit pure quaternion. The right pseudo-rotation of  $q$  by  $p$  is used here as an example.

$$\begin{aligned} \text{PRQ}_r(q, p) &= (ir + jg + kb)(ix + jy + kz) \\ &= -(rx + gy + bz) + i(gz - by) \\ &\quad + j(bx - rz) + k(ry - gx). \end{aligned} \quad (13)$$

Then the phase of  $\text{PRQ}_r(q, p)$  is

$$\theta = \tan^{-1} \left( -\frac{\sqrt{(gz - by)^2 + (bx - rz)^2 + (ry - gx)^2}}{rx + gy + bz} \right). \quad (14)$$

Observing the denominator of Eq. (14), it actually is the inner product of two vectors:  $(r, g, b)^T$  and  $(x, y, z)^T$ . If the quaternion  $q$  is closed (or similar) to the reference one  $p$ , the inner product will be large. On the other hand, the numerator of Eq. (14) consists of three parts, and each part is the difference of cross multiplications of two components of  $q$  and  $p$ . As a result, the differences of all the components of  $q$  and  $p$  in an overall way. If  $q$  and  $p$  are closed (or similar), the numerator of Eq. (14) is small. In a word, the closer  $q$  and  $p$  are, the larger value the phase has.

Take the first image in Fig. 1 as an example. After quaternion representation, we perform PRQ to each pixel by the reference quaternions  $i$ ,  $j$ , and  $k$ , then compute their phases. The results are shown in the first row in Fig. 2. The black points in the images are corresponding to the black points in the original image because the phase of black points is always zero. We can find that different reference quaternions will result in different phase images, and different color features of the original image can be seen.

Let us go back to the ranking of two quaternions  $q_i$  and  $q_j$ . We first apply them a PRQ by a given reference  $p_1$ , and then make a ranking decision according to the phase of two pseudo-rotated quaternions. The ranking function  $R(q_i, q_j)$  can be expressed as

$$R(q_i, q_j) = \theta_{\text{PQR}(q_j, p_1)} - \theta_{\text{PQR}(q_i, p_1)}. \quad (15)$$

It is possible to get different ranking results of  $q_i$  and  $q_j$  using different reference quaternions. This may help to understand the content of image information with different perspectives.

### 3.4. QLBP

To perform QLBP coding, the color image is first represented in a quaternionic way. Without loss of generality, we apply the most commonly used way:  $ir + jg + kb$  to represent the color pixel in the RGB color space. Consider an image pixel  $x_i$  centered in a  $3 \times 3$  block  $S_i$  and a previously specified reference quaternion  $p_1$ . The QLBP coding is obtained in the following way:

$$\text{QLBP}_{x_i} = \sum_{j=0}^{|S_i|-1} h(R(q_i, q_j))2^j, \quad (16)$$

where  $|S_i|$  is the number of elements in  $S_i$ ,  $h(\cdot)$  and  $R(q_i, q_j)$  are as defined in Eq. (5) and Eq. (15).

Images shown in the second row of Fig. 2 are the QLBP coding results of the first image in Fig. 1. We can find that the results are obviously different using different reference quaternion. Various local texture features are represented which may help to improve the reidentification results.

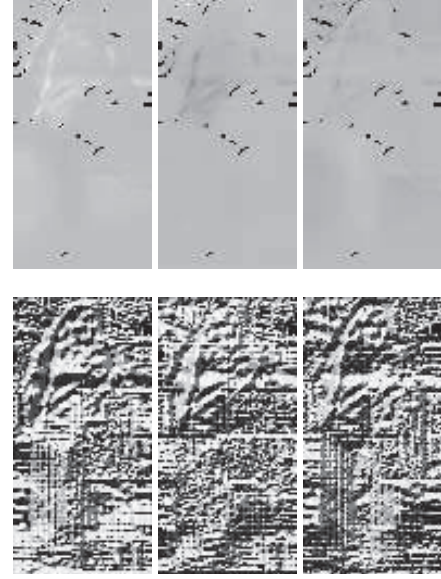


**Fig. 2:** Phase images and their corresponding QLBP coding results of the first image in Fig. 1 by using  $i$ ,  $j$ , and  $k$  as reference quaternions respectively.

## 4. FEATURE REPRESENTATION USING QLBP

The histogram of the QLBP coding image is used as features for person reidentification in this paper. To get more robust features against variations of the illumination, view angle, pose, and occlusion, the histogram is extracted from some overlapping cells. The centers of all cells are uniformly distributed in the image. A normalization is then performed to the histograms of all cells. Finally, concatenating the normalized histograms generates the QLBP feature representation of the original color image. The detailed steps are given in Algorithm 1.

---

#### Algorithm 1 QLBP feature extraction

**Input:** The color image  $I$ , a reference quaternion set  $\{p_1, p_2, \dots, p_L\}$ , and the sidelength of the local cell  $d$ .

- Step 1: Represent all pixels of  $I$  using Eq. (2). Denote the quaternionic image as  $Q_I$ .
- Step 2: For  $i = 1$  to  $L$ , do
  - (a) Perform PRQ to all the elements of  $Q_I$  by  $p_i$ , then calculate the phases of the rotated quaternionic image  $\text{PRQ}(Q_I, p_i)$ .
  - (b) Perform the QLBP coding according to Eqs. (15) and (16).
  - (c) Divide the QLBP coding image into several overlapping cells according the sidelength  $d$ .
  - (d) Calculate the histogram of each cell. List all histograms together to obtain a feature vector  $f_i$ .

**Output:** The QLBP feature vector of  $I$ :  $\{f_1, f_2, \dots, f_L\}$ .

---

## 5. EXPERIMENTS

In this section, several experimental results are provided to demonstrate the effectiveness of the proposed QLBP feature for person reidentification.

### 5.1. Experimental setting

Two commonly used datasets, ETHZ [12]<sup>1</sup> and i-LIDS Multiple-Camera Tracking Scenario (MCTS) [13, 14]<sup>2</sup>, are selected for evaluation. All images are normalized to size of  $128 \times 64$ . The proposed QLBP is compared with the LBP-based methods and other existing approaches for person reidentification: The traditional LBP [9], completed LBP (CLBP) [11], histograms of oriented gradient (HOG) descriptor [4], and Zheng's method [1]. For LBP and CLBP, features are extracted from the red, green, and blue components respectively. Similar operations are used for the HOG descriptor. The Zheng's method extracts features from both the color and texture information of the original images, and the obtained features are available online<sup>3</sup>.

In our experiments, all images of  $N$  persons are randomly chosen from the original dataset to form a test set. The test set is further divided into two parts: a gallery set and a probe set. Note that there is one image for each person in the gallery set, and the rest of images forms the probe set. Two images are considered to be the same person if they have the smallest  $l_1$ -norm distance. The average cumulative match characteristic (CMC) [1] is used to illustrate the ranked matching rates over 10 times of repeated matching. A matching rate of the top rank score  $r$  means the correct reidentification is obtained from the top  $r$  ranks with respect to  $N$  gallery images.

### 5.2. Simulation results

#### 5.2.1. ETHZ dataset

The ETHZ dataset contains 8580 images in total for 146 persons, and images of each person were taken from different view angles. Fig. 3 plots the CMC curves of  $N = 60$  and  $N = 120$  with different rank scores for all test methods. Observing Fig. 3(a), we can find that the matching rate of LBP is far less than all other methods. Considering the top 1 rank, the matching rates of QLBP is about 20% higher than LBP. HOG works better than the CLBP and Zheng's method but it is about 5% less than QLBP. As the number of top rank score increases, the Zheng's method outperforms HOG and is approaching to QLBP. In larger rank scores, the matching rates of HOG and CLBP are similar. Fig. 3(b) shows the results when the number of persons in the test images increases to 120. The proposed QLBP outperforms other methods and achieves the highest matching rates for all top rank score.

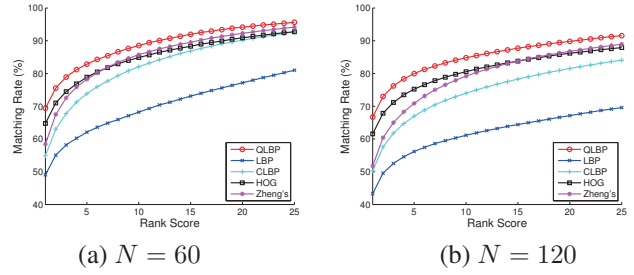


**Fig. 3:** CMC comparison results of different feature extraction methods on the ETHZ dataset.

When  $r$  is smaller than 15, HOG achieves better matching results. If  $r$  is larger than 15, the Zheng's method is slightly higher than HOG. The CLBP performs better than LBP but much less than QLBP. More detailed quantitative results are given in Table 1 with  $N$  is set to be 40, 80, and 120 respectively.

#### 5.2.2. i-LIDS MCTS dataset

The i-LIDS MCTS dataset was obtained indoor at a airport arrival hall. This dataset is composed of 476 person images for 119 people, and all images are captured by multiple nonoverlapping cameras for each person.

Fig. 4 shows the CMC curves of  $N = 40$  and  $N = 80$  with different rank scores for all test methods. First let us see the results of  $N = 40$ . When  $r$  equals to 1, LBP, CLBP, and HOG obtain similar matching results. The QLBP outperforms these methods about 3%, while the Zheng's method gets the worst results. As the top rank score increases, the matching rate of all methods increases. The proposed QLBP is superior to all other methods. For most situations, there is no obvious distinction between LBP and CLBP. The performance of the Zheng's method is close to HOG while the top rank score increases. For the largest top rank score, the differences of the matching rates of all methods are small. As shown in Fig. 4(b), the matching rates of QLBP are much better than those of all other methods when the number of persons increases to 80. Table 1 gives detailed quantitative results with the person number is chosen as 30, 60, and 90 respectively.

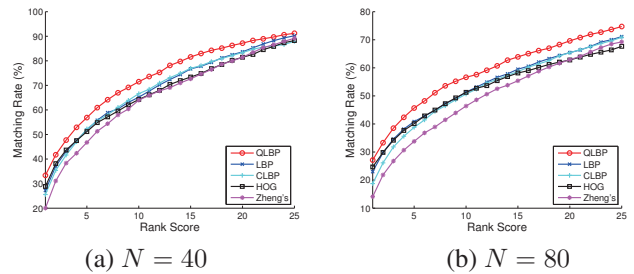


**Fig. 4:** CMC comparison results of different feature extraction methods on the i-LIDS dataset.

<sup>1</sup><http://www.umiacs.umd.edu/~schwartz/datasets.html>.

<sup>2</sup><http://www.eecs.qmul.ac.uk/~jason/>

<sup>3</sup><http://www.eecs.qmul.ac.uk/~jason/ilids.html>.

**Table 1:** Top Ranked Matching Rate (Percent) on ETHZ and i-LIDS MCTS Datasets

Methods	ETHZ Dataset											
	N = 40				N = 80				N = 120			
	r=1	r=5	r=15	r=20	r=1	r=5	r=15	r=20	r=1	r=5	r=15	r=20
QLBP	<b>70.30</b>	<b>84.89</b>	<b>90.59</b>	<b>95.85</b>	<b>67.20</b>	<b>81.45</b>	<b>86.52</b>	<b>91.57</b>	<b>66.69</b>	<b>79.97</b>	<b>84.80</b>	<b>89.81</b>
LBP	49.70	63.24	71.48	82.09	46.59	58.92	64.45	72.06	43.33	56.16	61.14	67.15
CLBP	57.08	77.40	85.96	93.99	52.56	70.82	78.46	86.32	50.24	66.98	73.99	81.52
HOG	65.30	81.25	87.47	93.58	62.23	76.39	82.20	88.10	61.57	75.23	80.56	86.19
Zheng's	55.71	78.89	87.33	95.22	52.64	72.99	81.25	89.16	51.75	70.88	79.20	86.76

Methods	i-LIDS Dataset											
	N = 30				N = 60				N = 90			
	r=1	r=5	r=15	r=20	r=1	r=5	r=15	r=20	r=1	r=5	r=15	r=20
QLBP	<b>31.57</b>	<b>57.79</b>	<b>74.39</b>	<b>92.02</b>	<b>28.58</b>	<b>49.32</b>	<b>62.94</b>	<b>77.28</b>	<b>24.91</b>	<b>43.26</b>	<b>54.04</b>	<b>66.87</b>
LBP	28.20	52.97	70.64	90.73	23.98	44.61	57.08	73.36	21.51	39.04	48.90	61.92
CLBP	25.92	50.43	67.45	87.79	22.78	44.15	58.28	73.45	19.29	37.35	47.33	60.75
HOG	29.20	52.11	69.16	88.52	26.52	44.88	54.52	67.27	23.04	37.54	47.35	59.07
Zheng's	21.97	50.28	68.07	88.34	16.38	37.90	52.35	68.91	12.84	32.05	44.14	60.23

## 6. CONCLUSIONS

In this paper, we developed a quaternionic local binary pattern (QLBP) for person reidentification. Unlike most existing methods which usually extract features from each color channel of original image, the proposed QLBP makes use of quaternion to represent each color pixel such that we can handle all color components at one time. A pseudo-rotation of quaternion (PRQ) was proposed to rank two quaternions, then the local binary pattern coding was implemented to extract features. Experiments were carried out to evaluate the proposed QLBP, and promising results have been achieved.

## 7. REFERENCES

- [1] W. Zheng, S. Gong, and T. Xiang, “Reidentification by relative distance comparison,” *IEEE Trans. Pattern Anal. Mach. Intell.*, vol. 35, no. 3, pp. 653–668, 2013.
- [2] X. Liu, M. Song, D. Tao, X. Zhou, C. Chen, and J. Bu, “Semi-supervised coupled dictionary learning for person re-identification,” in *Proc. IEEE Int. Conf. Comput. Vis. Pattern Recognit.*, 2014.
- [3] K. Sande, T. Gevers, and C. Snoek, “Evaluating color descriptors for object and scene recognition,” *IEEE Trans. Pattern Anal. Mach. Intell.*, vol. 32, no. 9, pp. 1582–1596, 2010.
- [4] N. Dalal and B. Triggs, “Histograms of oriented gradients for human detection,” in *Proc. IEEE Int. Conf. Comput. Vis. Pattern Recognit.*, 2005.
- [5] M. Farenzena, L. Bazzani, A. Perina, V. Murino, and M. Cristani, “Person re-identification by symmetry-driven accumulation of local features,” in *Proc. IEEE Int. Conf. Comput. Vis. Pattern Recognit.*, 2010.
- [6] I. Kviatkovsky, A. Adam, and E. Rivlin, “Color invariants for person reidentification,” *IEEE Trans. Pattern Anal. Mach. Intell.*, vol. 35, no. 7, pp. 1622–1634, 2013.
- [7] T. Ell and S. Sangwine, “Hypercomplex Fourier transforms of color images,” *IEEE Trans. Image Process.*, vol. 16, no. 1, pp. 22–35, 2007.
- [8] S. Sangwine, “Fourier transforms of colour images using quaternion, or hypercomplex, numbers,” *Electron. Lett.*, vol. 32, no. 21, pp. 1979–1980, 1996.
- [9] T. Ojala, M. Pietikainen, and T. Maenpaa, “Multiresolution gray-scale and rotation invariant texture classification with local binary patterns,” *IEEE Trans. Pattern Anal. Mach. Intell.*, vol. 24, no. 7, pp. 971–987, 2002.
- [10] W. Hamilton, “Elements of quaternions,” London, U.K.: Longmans Green, 1866.
- [11] Z. Guo, L. Zhang, and D. Zhang, “A completed modeling of local binary pattern operator for texture classification,” *IEEE Trans. Image Process.*, vol. 19, no. 6, pp. 1657–1663, 2010.
- [12] A. Ess, B. Leibe, and L. Gool, “Depth and appearance for mobile scene analysis,” in *Proc. IEEE Int. Conf. Comput. Vis.*, 2007.
- [13] UK, “Home office i-LIDS multiple camera tracking scenario definition,” 2008.
- [14] W. Zheng, S. Gong, and T. Xiang, “Associating groups of people,” in *British Mach. Vis. Conf.*, 2007.